Autonomous Imagination: Closed-Loop Decomposition of Visual-to-Textual Conversion in Visual Reasoning for Multimodal Large Language Models

Anonymous authors
Paper under double-blind review

Abstract

Under pure textual modality, Large Language Models (LLMs) have demonstrated remarkable success in complex reasoning tasks by decomposing them into simpler sub-problems. However, Multimodal Large Language Models (MLLMs) still struggle with some seemingly straightforward visual tasks, such as counting and solving jigsaw puzzles. We argue that these tasks challenge the ability of *visual-to-textual conversion*, where MLLMs convert visual information perceived from the input scene, to textual information for further reasoning and generating the answer. If the complexity of the visual input is beyond the perceptual capability of the MLLMs, without decomposing this conversion process, simply scaling inference-time reasoning cannot solve the task because it repeatedly encounters the same perceptual bottleneck. We propose an approach, *autonomous imagination*, to enable MLLMs to iteratively modify visual inputs (e.g. isolating objects, rearranging puzzle pieces) into intermediate visual states, decomposing visual-to-textual conversion into closed-loop visual modification steps. We show that, without any retraining, MLLMs can now solve tasks initially beyond their perceptual capability, highlighting that closed-loop visual modification can be an effective way of decomposing the visual reasoning task into solvable substeps. Our code and data are released at (publicly available upon acceptance).

1 Introduction

Modern Large Language Models (LLMs) demonstrate exceptional reasoning capabilities through systematic task decomposition (Huang & Chang, 2023). By breaking complex problems into sequential subtasks, models achieve remarkable performance in textual reasoning domains (Yao et al., 2023; OpenAI, 2024b). More recently, Multimodal Large Language Models (MLLMs) (OpenAI, 2024a; Liu et al., 2023; Bai et al., 2023; Wang et al., 2023a) are gaining increasingly strong abilities in visual understanding. Inspired by work on visual prompting (Jiang et al., 2024; Lin et al., 2024; Hong et al., 2023; Zhang et al., 2023b;c; Mitra et al., 2023; Zheng et al., 2023; Zhang et al., 2024; Yu et al., 2024), recent methods enable MLLMs to perform visual reasoning by proactively adding visual prompts (such as bounding boxes) to the image, to reduce hallucination and handle challenging visual tasks without human intervention (Lai et al., 2023; Wu & Xie, 2023; Chen et al., 2023; Qi et al., 2024; Shao et al., 2024; Zhou et al., 2024b).

Despite these advancements, existing methods often struggle to make MLLMs natively handle intuitive visual reasoning tasks. When challenged with tasks such as jigsaw puzzle assembly (even when provided with explicit step-by-step instructions), or simply counting objects, state-of-the-art MLLMs consistently fail to reason through the entire process. A key observation is that, instead of challenging high-level reasoning abilities such as logical deduction, these tasks actually challenge the ability to perceive and understand complex visual scenes. Referring to the failure of existing MLLMs on them, we argue that ineffective task decomposition remains a fundamental cause. Reasoning in complex visual input requires the strong ability of *visual-to-textual conversion*, where MLLMs convert visual information perceived from the input scene to textual information for further reasoning and generating the answer. However, in current MLLM reasoning, the visual-to-textual conversion process remains an atomic operation rather than being divided

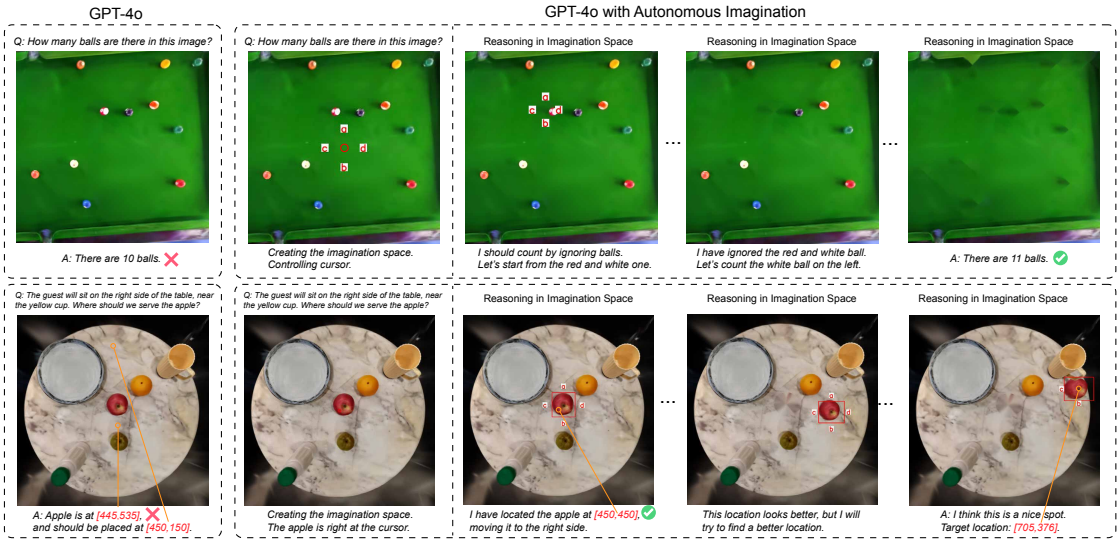

Figure 1: Our autonomous imagination approach empowers advanced MLLMs to engage in iterative imaginative reasoning, enabling them to address previously unsolvable tasks without additional training.

into executable substeps. When the complexity of the visual scene is beyond the perceptual ability of MLLMs, without decomposing this conversion step, simply scaling inference-time reasoning cannot solve the task because it repeatedly encounters the same perceptual bottleneck.

We hypothesize that, similar to textual reasoning, where intermediate textual states are necessary, MLLMs need to generate intermediate images that gradually simplify the original scene or approach the target visual state. To test this, we propose enabling MLLMs to iteratively modify visual inputs (e.g., isolating objects, rearranging puzzle pieces) into intermediate visual states, decomposing visual-to-textual conversion into closed-loop visual modification steps, without any additional training of MLLMs. For simplicity, we refer to this approach as *autonomous imagination*. Technically, we implement the approach to support the conversion from an unstructured input visual scene into a structured representation and the visual operators that efficiently modify the visual content into new states (e.g., through transformation or erasing). This allows MLLMs to generate successive visual states that progressively simplify the original visual scene or gradually approach the target visual state in an autonomous fashion.

We conduct experiments under visual reasoning tasks that challenge the perception and understanding abilities of MLLMs under complex visual scenes, including counting, jigsaw puzzle solving, object placement, and multi-object hallucination. The results show that previously challenging visual reasoning tasks, which are beyond the perceptual capability of the MLLMs, can be effectively tackled natively by them equipped with our approach. This serves as empirical validation that a major limitation in visual reasoning stems from insufficient support for visual task decomposition, which we hope will inspire future research.

2 Related Work

2.1 Reasoning in LLMs

Numerous studies explore reasoning paradigms in natural language using their in-context learning ability (Brown et al., 2020), showing that Large Language Models (LLMs) improve through reasoning-based outputs (Wei et al., 2022; Kojima et al., 2022). Subsequent work further improves reasoning through in-context learning by improving in-context sample selection (Rubin et al., 2021; Lu et al., 2022; Zhang et al., 2022; Fu et al., 2022; Wang et al., 2022; Li et al., 2022b). Recently, notable advancements in OpenAI's o1 (OpenAI, 2024b) have demonstrated that by scaling LLMs for inference-time reasoning before answering,

LLMs can be greatly enhanced in reasoning. A key insight from these advances is that proper decomposition of the reasoning process into simpler subtasks is essential for successful reasoning (Wei et al., 2022).

2.2 Visual Reasoning in MLLMs

MLLMs have evolved in visual understanding ability, initially leveraging domain-specific expert models such as HuggingGPT (Shen et al., 2023), MM-REACT (Yang et al., 2023), and VisualChatGPT (Wu et al., 2023). The focus later shifted to training LLMs with an adapter for the other modal, such as LLaVA (Liu et al., 2023), BLIP-2 (Li et al., 2022a; 2023), and MoVA (Zong et al., 2024). Many recent MLLMs now exhibit native visual understanding through training in text-image pairs, with fine-tuning on question-answering tasks (Liu et al., 2023; Bai et al., 2023; Wang et al., 2023a; Zhu et al., 2023; Chen et al., 2022; Luo et al., 2023; Alayrac et al., 2022), including the state-of-the-art closed-source MLLM GPT-4o (OpenAI, 2024a).

In addition to reasoning within text modalities, substantial efforts are made in reasoning in visual tasks. Existing MLLMs often face limitations in direct visual perception and are prone to generating answers with hallucinations (Zhang et al., 2023d). Initial approaches used attention mechanisms to improve question-answering abilities (Zhou et al., 2021), and subsequent solutions include strengthening reasoning in the visual modality by training (Lin et al., 2023; Wang et al., 2023b) or employing auxiliary knowledge (Mitra et al., 2023). In addition, researchers have proposed effective visual prompting methods to refine the focus of MLLMs (Jiang et al., 2024; Lin et al., 2024; Hong et al., 2023; Zhang et al., 2023b;c; Mitra et al., 2023; Zheng et al., 2023; Zhang et al., 2024; Yu et al., 2024). See Wu et al. (2024a) for the recent comprehensive survey. Attempts have been made to utilize visual prompts in the Chain-of-Thought (CoT) paradigm (Wei et al., 2022). Based on pioneer studies (Zhang et al., 2023d; Zheng et al., 2023; Zhang et al., 2023a; Peng et al., 2023), recent approaches build CoT by enabling MLLMs to add visual prompts autonomously either through direct model training (Lai et al., 2023; Wu & Xie, 2023; Chen et al., 2023; Qi et al., 2024; Shao et al., 2024) or by utilizing external visual processing models (Zhou et al., 2024b). By using visual prompts (e.g., bounding boxes) to highlight key information in images, the visual-to-textual conversion step becomes easier, leading to a performance boost. However, even though visual prompts simplify the perception of input images, this paradigm still restricts to do visual-to-textual conversion only in one step, which is after all visual prompts are added in the input. As our experiments demonstrate, even when visual prompting is applied, visual-to-textual conversion remains a bottleneck in common visual reasoning tasks that are intuitive to humans, highlighting the necessity of effective task decomposition.

We also discuss some recent work on action planning, which addresses a significantly different task from ours, while has also explored various imagination techniques, such as using video generation models to simulate control processes as references (Ajay et al., 2023; Du et al., 2023), employing image generation to visualize target goals (Zhou et al., 2024a), and improving an LLM's understanding of the current state, either through textual descriptions or visualizations (Liu et al., 2022; Wu et al., 2024b). However, these approaches are limited to closed-world settings where the state and action spaces are predefined. Although these techniques have shown promising results in closed environments, they are designed specifically for constrained settings and cannot be directly extended to open-world contexts, where the visual scene is primitive and unstructured.

The closest studies to ours are from the field of robotics, where recent methods utilize the ability of MLLMs to perform object manipulation (Kapelyukh et al., 2024; Ding et al., 2024). These methods also create a virtual space and use MLLMs as evaluators to judge whether the object's final state matches the instruction, in order to generate a final state where the object should be moved to. However, current approaches adopt random sampling to conduct exhaustive searches in the virtual environment, which is not feasible when the possible state space is large. We implement this method in the experiments to verify this argument.

3 Method

3.1 Problem Formulation

We challenge MLLMs with visual reasoning tasks that are intuitive for humans: *counting, jigsaw puzzle solving, object placement, and multi-object hallucination.* For object placement, to capture a holistic top-

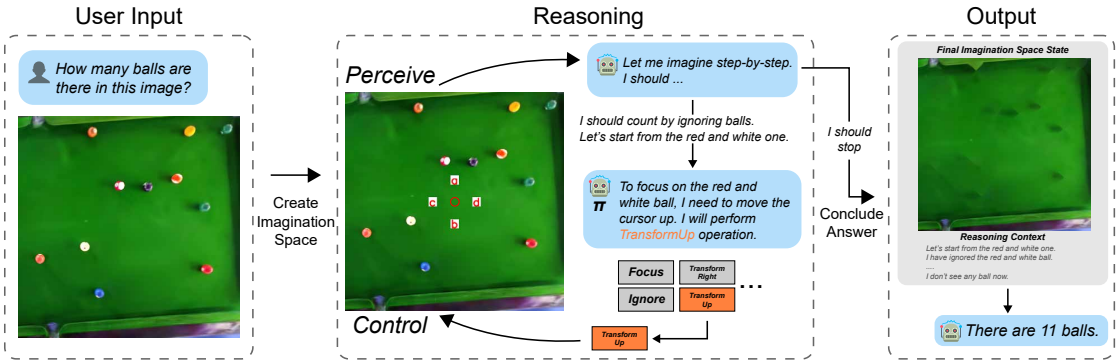

Figure 2: An overview of our autonomous imagination approach: The imagination space begins with an unstructured input scene and undergoes an iterative reasoning process. In each cycle, MLLMs first perceive the current state of the imagination space, select an operation to apply, and then reassess the updated imagination space. Upon completing this reasoning sequence, MLLMs generate an answer based on the cumulative context of the process and the final state of the imagination space.

down view, we reconstruct the input scene using 3D Gaussian Splatting (Kerbl et al., 2023) and render it from a top-down perspective. We directly feed the unstructured raw input scene into the model: no semantic pre-processing (e.g., segmentation or grounding) is applied initially, aligning with real-world settings where visual inputs are provided directly. We evaluate whether MLLMs can natively solve these tasks by proactively modifying the visual state on their own, with minimal reliance on external semantic visual understanding abilities (e.g., we avoid using object detection models for counting, which would constitute "cheating").

3.2 Closed-Loop Reasoning Formulation

To enable existing MLLMs to proactively modify the visual scene during reasoning, we propose a plug-and-play virtual space. In this framework, the MLLM is treated as a pre-trained policy that executes a sequence of operations. We refer to this space as the *imagination space* for simplicity. The MLLM can move a cursor to focus on an object, perform an operation on it (e.g., ignore or transform it), and then go back to use the cursor again until convergence. The imagination space continuously updates the MLLM with the latest visual state by dynamically re-rendering the scene.

Note that our only external model dependency is Segment Anything 2 (SAM2) (Ravi et al., 2024), which is invoked solely to isolate a visual element after the MLLM selects it via the cursor. Since our focus is on testing visual perception rather than high-level logical reasoning, we directly provide the MLLM with task-specific reasoning plans (e.g., "count by ignoring balls") through system prompts. This mitigates occasional failures caused by the MLLM adopting bad reasoning strategies.

Specifically, we assume that the MLLM is given an input image o and input text prompt token r_0, the aim of the reasoning is to obtain the prediction probability $P(y|o, r_0)$, where y is the final output text token. In general, to utilize CoT, the reasoning problem of predicting $P(y|o, r_0)$ can be transformed into intermediate steps of predicting $P(z_t|o, z_{t-1}), t \in 1, 2, \ldots, T$. Each $z_t = \{r_t, c_t\}$ denotes the augmented textual prompts r_t and visual information c_t for deepening scene understanding and pushing forward reasoning. After the final reasoning step at T, the final output is set to $y = r_T$. The target transforms into predicting the following joint probability:

$$P(z_{1:T}|o, r_0) = \prod_{t=1}^{T} P(z_t|o, z_{0:t-1}), \tag{1}$$

where $z_{t_1:t_2} = \{z_{t_1}, z_{t_1+1}, \ldots, z_{t_2}\}$ and $z_0 = r_0$. What is essential in CoT design is to make each step simple enough to match the reasoning capacity of MLLMs.

In imagination space, $\hat{o}$ are images rendered from the space for MLLMs to perceive. We also introduce a set of *operators* to modify the imagined scenes into new ones. Denote by $v_t = \{\hat{o}_t, r_{0:t}\}$ and a_t the operator in

step t. Our method transforms Eq. 1 into

$$P(\hat{o}_{1:T}, r_{1:T}, a_{1:T}|o, r_0) = \prod_{t=1}^{T} P(v_t, a_t|v_{t-1}), \tag{2}$$

where $v_0 = \{o, r_0\}$ and finally $y = r_T$. The one-step reasoning task $P(v_t, a_t|v_{t-1})$ is factorized into

$$P(v_t, a_t|v_{t-1}) = \pi(a_t|v_{t-1})\phi(\hat{o}_t|\hat{o}_{t-1}, a_t)\omega(r_t|\hat{o}_t, r_{0:t-1}). \tag{3}$$

Eq. 3 shows that one-step reasoning is factorized into a decision function $\pi(a_t|v_{t-1})$, a scene modification function $\phi(\hat{o}_t|\hat{o}_{t-1}, a_t)$, and a reasoning function $\omega(r_t|\hat{o}_t, r_{1:r-1})$. Given the current imagined scene $\hat{o}_{t-1}$ and the augmented text prompt token r_{t-1}, the decision function chooses a specific scene modification operator a_t. The scene modification function then utilizes a_t to update $\hat{o}_{t-1}$ into $\hat{o}_t$. The reasoning function finally updates r_{t-1} into r_t based on $\hat{o}_t$. The decision and reasoning functions are purely based on the native reasoning ability of MLLMs. The scene modification function is implemented inside the imagination space.

Comparing Eq. 1 and Eq. 2, the imagination space transforms CoT reasoning into a closed-loop decision-making and reasoning process. During the reasoning process, the visual state is gradually simplified or approaching a target visual state: the reasoning step at step t is only dependent on $\hat{o}_{t-1}, \hat{o}_t$ but independent of all previous visual states, leads to effective task decomposition.

3.3 Imagination Space

The imagination space is designed to render images for MLLMs to perceive and supports a minimal set of operators for MLLMs to call: focus, ignore, and transform. Focus isolates relevant content for further manipulation, ignore enables MLLMs to disregard extraneous information, and transform allows the repositioning of desired content. This compact set of operations enables MLLMs to reason and solve practical challenges by themselves, as demonstrated in our experiments. MLLMs select operators through natural language output, which are then applied to the imagination space. The updated space is rendered and returned to MLLMs for the subsequent reasoning step.

We discuss the detailed implementation of the operators in the following sections. The operators are implemented separately for the 2D space (represented as images) and the 3D space (represented via 3D Gaussians). MLLMs are unaware of this implementation difference, as it interacts exclusively with rendered images as input and executes operators identically in both scenarios.

3.4 Focus Operator

The focus operator allows MLLMs to isolate and label target content from a scene, creating distinct elements for further transformation. Once MLLMs identify an object of interest using a virtual cursor (as described in Sec. 3.7), the focus operator segments this content for focused manipulation. In 2D space, this cursor directly conditions the Segment Anything Model (SAM) (Kirillov et al., 2023) to perform segmentation. MLLMs verify segmented output to ensure alignment with their intended focus. In the 3D Gaussian space, segmentation on demand poses unique challenges: Existing methods (Ye et al., 2024; Shen et al., 2024) are designed for unconditional segmentation, where all objects are segmented without the ability to specify conditions. However, our use case requires conditional segmentation, focusing on a specific object selected by an input condition, making these methods unsuitable.

To enable the focus operator in 3D Gaussian-based representations, we introduce a method to selectively segment an object from an unstructured 3D Gaussian scene, which is illustrated in Alg. 1. Given the MLLM's initial selection block, we first generate a virtual camera trajectory that orbits around the targeted object, creating a video sequence. This sequence is fed into the SAM2 model (Ravi et al., 2024), which applies the selection cursor condition on all rendered frames. For each frame, rays are cast from pixels within the segmentation mask, and path tracing records the radiance contributions of intersecting Gaussians. This process is expressed as volumetric integration illustrated in Line 4-11. Gaussians who receive a contribution higher than a threshold will receive one vote.

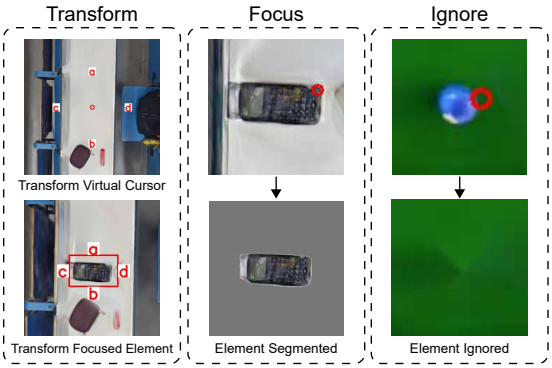

Figure 3: Illustrations of operations within our imagination space: transformations can be applied to focused elements (including the virtual cursor), focus operations allow segmentation of cursor-selected elements, and ignore operations make cursor-selected elements visually invisible.

Algorithm 1: 3D conditional segmentation

Input : SAM2 mask, 3D scene, thresholds ϵ_1, ϵ_2
Output: Set of marked Gaussians $\mathcal{G}_{\text{marked}}$

Initialize vote counts: votes$[g_i] \leftarrow 0$ for each Gaussian g_i in the scene
foreach *pixel p in masked_pixels* **do**
  ray $\leftarrow$ cast_ray(p) ; $T \leftarrow 1$
  foreach *Gaussian g_i intersected by ray* **do**
    $\alpha_i \leftarrow$ get_alpha(g_i, ray) ; $C_i \leftarrow T \cdot \alpha_i$
    if $C_i > \epsilon_1$ **then**
      votes$[g_i] \leftarrow$ votes$[g_i]$ +1
    end
    $T \leftarrow T \cdot (1 - \alpha_i)$
    if $T < \epsilon_2$ **then break**
  end
end
max_vote $\leftarrow$ maximum of votes$[g_i]$ over all g_i
$\mathcal{G}_{\text{marked}} \leftarrow \emptyset$
foreach *Gaussian g_i* **do**
  if *votes$[g_i] \geq 0.1\times$ max_vote* **then**
    $\mathcal{G}_{\text{marked}} \leftarrow \mathcal{G}_{\text{marked}} \cup \{g_i\}$
  end
end

We select the 3D Gaussian with votes exceeding 10% of the highest vote, forming a shell around the target object's radiance field. This shell, along with the internal radiance Gaussians, is segmented collectively to define the object's radiance structure. In both 2D and 3D spaces, the segmented object is placed in a separate layer, while the remaining content is retained in a base layer.

3.5 Ignore Operator

The ignore operation removes a focused object from the imagination space to prevent interference with the reasoning process. Since API access to state-of-the-art MLLMs does not support attention masks, removing the object leaves a hole in the base layer, potentially causing hallucinations. To address this, we simply inpaint the hole created by the removal of the object. For both 2D and 3D imagination spaces, we project the object mask onto the rendered image as the region to inpaint. We directly use the implementation provided by OpenCV (Itseez, 2015) by simply merging the nearby pixels. The inpainted image is then used

for further reasoning by the MLLMs, avoiding paying attention to the inpainted region as the content has been removed.

3.6 Transform Operator

Object transformation can occur in four directions: up, down, left, and right, each represented by an alphabet character (a, b, c, d) to avoid interference with semantically meaningful words. In each step of the iterative imagination process, MLLMs select a direction for movement. Since MLLMs struggle with determining precise distances, we standardize movement units in screen space coordinates and gradually reduce step size throughout the process, where MLLMs only control the direction of movement.

3.7 Reasoning Process

The iterative reasoning process described in Sec. 3.2 is executed as follows: After initializing the imagination space, a virtual cursor is positioned at the center and automatically considered as focused. MLLMs can perform transform operations on the cursor to reposition it within the space. Following each operation, MLLMs conduct scene modification and receive an updated image of the newly rendered imagination space.

When MLLMs identify that the cursor has selected a visual element of interest, a focus operation is performed based on the location of the cursor. If MLLMs determine that this operation has correctly segmented the intended element, the focus is shifted to that object, enabling MLLMs to execute either a transformation or ignore operation on it. Once MLLMs have either repositioned or disregarded the object, the focus returns to the virtual cursor. This process iterates continuously as part of the reasoning workflow until all necessary reasoning steps are completed, culminating in a final textual response.

4 Experiments

In the experiments, we challenge MLLMs with four tasks that are intuitive to humans and require strong visual understanding and reasoning abilities: counting, simple jigsaw puzzle solving, object placement, and multi-object hallucination. We target at verifying that compared to 1) simply scaling textual reasoning steps 2) conducting visual prompting, while still conducting visual-to-textual conversion within a single step, the closed-loop task decomposition paradigm is indeed more effective and necessary.

4.1 Benchmark and Evaluation Protocol

Counting: When faced with numerous densely packed objects, humans often rely on multi-step reasoning to reach an accurate count, as a single glance may not suffice. Existing MLLMs, however, struggle with counting, as their multistep reasoning is not yet effective for this task. We include this task to assess whether the model can leverage reasoning to offset its limited direct perception, mirroring human strategies.

For evaluation, we directly compare the predicted count of the model with the ground truth. In addition to reporting the **success rate**, we calculate the **mean** and **variance** of the counting errors to provide insight into the accuracy and consistency of each approach. We constructed 122 images with real objects with paired ground truth.

Solving Simple Jigsaw Puzzles: Jigsaw puzzles are classic tests of visual perception and reasoning, commonly used to assess intelligence. In this task, we evaluate the ability of MLLMs to solve simple jigsaw puzzles, aligning their problem-solving performance with that of humans to assess visual reasoning capabilities. In the jigsaw puzzle solving task, MLLMs are tasked with identifying and placing missing pieces in their correct locations.

For evaluation, we use a digital jigsaw puzzle game with a magnetic mechanism, where pieces automatically snap into place when positioned close to their correct locations. Success is measured by the **completion rate**, defined as the percentage of pieces placed in their correct locations. For evaluation, we constructed 11 cases where four pieces are missing and 11 cases where six pieces are missing. The size of the puzzle ranges from 3×5 to 5×8.

Object Placement: Previous methods have shown progress in enabling MLLMs to understand and describe static scenes, such as identifying object locations (e.g., "Where is the cup?"). However, for practical use, MLLMs must also interpret dynamic instructions that convey intent, such as "Where should the cup be placed?" In the object placement task, MLLMs are required to identify both the current and target locations of objects based on abstract instructions (e.g., "Prepare two cups for guests in the living room"). Given the input scene of 3D Gaussians, MLLMs must determine the original locations of objects and their intended locations based on a provided prompt.

For evaluation, we first measure the **locating success rate**, which reflects the model's ability to accurately identify the initial location of the correct object. If the model fails to do this, the placement task is automatically marked as a failure. We then measure the **placement success rate** by checking whether the predicted final location falls into the marked ground-truth region. For both success rates, when multiple correct solutions exist, we provide multiple ground truth regions and selecting any valid region is considered correct. We captured a total of 17 scenes, including 271 user prompts and paired ground truth for evaluation.

Multi-Object Hallucination: Current MLLMs can suffer from hallucination by perceiving or generating non-existing objects in the input scene. The complexity of the input scene is beyond the limitation in perceptual capability of MLLMs, which is a plausible reason for hallucination. Our approach can serve as a promising way to address this challenge, especially for the scenes where multiple objects exist. By the closed-loop iterative process of autonomous imagination, MLLMs can deal with objects one by one, as in our counting benchmark, instead of handling them all together, effectively reducing the possibility of hallucination. We conducted additional experiments on the recently proposed multi-object hallucination benchmark ROPE (Chen et al., 2024) to validate this argument. We focus on the most challenging subset in the benchmark where the state-of-the-art model on the official leaderboard, GPT-4o, exhibits the poorest performance, which is answering about single object given multiobject image, heterogeneous object types, on unseen data split. We refer to the detailed benchmark setting from the original paper.

4.2 Baselines

We evaluate our approach against state-of-the-art MLLM, namely **GPT-4o** (OpenAI, 2024a) (our approach is also utilized to enhance GPT-4o in all experiments). We provide a clearly defined 2D coordinate system to GPT-4o so that output coordinates are generated without any ambiguity. We also adopt the recently proposed visual reasoning method **VCoT** (Shao et al., 2024) using their open-released pre-trained model. We developed a baseline **GPT-4o Sampling** inspired by the sample-then-evaluate imagination paradigm used in robotics (Kapelyukh et al., 2024; Ding et al., 2024). Since their original methods are designed for robotic manipulation, we reimplement them under our method. Note that this sampling strategy can only be applied to some of the tasks in our evaluation since sampling in large solution spaces is heavily intractable. Furthermore, to demonstrate the necessity of altering the visual scene for task decomposition beyond adding visual prompts, we crafted a reasoning baseline named **cursor-only** that utilizes our imagination space, but restricts operations solely to transform operations of the virtual cursor. Note that this baseline serves as an ablation of our method, which has the same closed-loop control design except that scene modification is disabled and only virtual cursor moving is enabled. Furthermore, we also adopt two recently proposed advanced MLLMs, namely **OpenAI's o1** (OpenAI, 2024b) and **Molmo** (Deitke et al., 2024). o1 is well known to have specifically trained reasoning abilities under pure textual modality. We utilize it to justify whether simply scaling text-time textual reasoning could solve the tasks. On the other hand, Molmo is trained to have ability to utilize visual markers as cues in visual modality for reasoning. We utilize it to justify the necessity of task decomposition instead of conducting visual prompting with visual markers.

4.3 Counting

The results are shown in Tab. 1. Our approach significantly improves the performance of original GPT-4o, achieving a higher success rate and lower errors when mistakes occur. It is worth noting that Molmo is known to be specifically trained to conduct counting with its native "pointing" ability. Our approach enables GPT-4o to perform on par with it. Note that the sampling method is not directly applicable to the counting task due to intractability, so we omit its comparisons. VCoT only supports drawing one bounding box to

Table 1: Quantitative comparison results under counting, jigsaw puzzle solving, and object placement. See Sec. 4.1 for details of the metrics. We consider two variants of cursor-only in counting, leading to two sets of results, and GPT-4o Sampling cannot be applied to counting and locating as illustrated, please see Sec. 4.3, 4.2, and Sec. 4.5 for details. *In object placement, cursor-only functions the same as our method in locating, so their results are identical. Furthermore, NA* indicates that under these tasks, Molmo constantly fails to output reasonable coordinates or refuses to output.

Settings		GPT-4o	o1	Molmo	VCoT	Ours (cursor-only)	GPT-4o Sampling	**GPT4o+Ours**
Counting	Success Rate	39.8%	50.8%	**86.2%**	15.5%	39.0%/0%	-	85.3%
	Mean Error	0.73	0.74	0.34	3.11	1.12/*not calculable*	-	**0.19**
	Variance	0.62	0.90	2.57	5.51	1.22/*not calculable*	-	**0.22**
Simple Jigsaw Puzzle	4-Piece Missing	29.5%	31.8%	NA*	9.1%	27.3%	43.2%	**68.2%**
	6-Piece Missing	9.1%	27.3%	NA*	3.3%	24.2%	30.3%	**51.5%**
Object Placement	Locating	10.9%	17.3%	NA*	10.4%	**69.4%***	-	**69.4%**
	Placement	3.6%	8.5%	NA*	1.5%	27.8%	17.3%	**37.3%**

highlight a piece of visual evidence, hence is unsuitable for more complex reasoning tasks involving multiple objects, such as counting. We also compare with our cursor-only baseline in counting, observing that it performs similarly to GPT-4o. Since having a cursor moving around might be ineffective for counting, we adopt a cursor-only variant, where the MLLM can draw a bounding box on the cursor location to highlight the object during counting. Although technically able to draw boxes on every ball to perform counting accurately, the model quickly enters a negative feedback loop: hallucinations lead it to draw more markers, which introduce additional noise and exacerbate the hallucinations. This results in a success rate of 0% and makes mean error and variance not calculable, as the model cannot stop counting, further highlighting the importance of modifying the visual scene.

To further verify the essentialness of task decomposition in visual modality, we conduct additional analysis under the real object data by increasing the counting difficulty by adding more objects with partial data. The purpose was to evaluate the impact of difficulty and reasoning steps on performance. To achieve this, we selected a subset of cases from the whole data and supplemented them with simpler cases involving fewer objects. We then re-conducted the experiments on this partial dataset using GPT-4o, alongside a newly introduced textual CoT reasoning baseline. In the first experiment (Fig. 4a), we show the success rate of different methods when faced with varying numbers of objects. In the second experiment (Fig. 4b), we test how different methods improve when given different limits on the number of reasoning steps. The result is shown as the solvable rate, which indicates the percentage of cases the method can solve under the current budget. When imposing such a limit, our model is restricted to performing no more than the specified number of steps, with each step defined as a combination of the focus operation and the subsequent operation performed after focusing. For the textual CoT baseline, we explicitly instructed the model on the maximum number of reasoning steps it was allowed to use. The results are shown in Fig. 4a with an additional baseline **GPT-4o-text-cot**, indicating the pure text-based CoT. This reveals perceptual limitations in GPT-4o that cannot be overcome by simply increasing the textual CoT steps, while our method remains unaffected. Fig. 4b shows the percentage of cases solved as reasoning steps increase. For reference, we include the one-step results from GPT-4o depicted as a flat line. Our method performs consistently better as reasoning steps grow, whereas GPT-4o-text-cot fails to do this and may even introduce noise, resulting in poorer performance than one-step GPT-4o.

4.4 Simple Jigsaw Puzzle Solving

In the jigsaw puzzle solving task, the rotations of pieces are not considered. As multiple trials are allowed, we restrict the total number of attempts to 20 and report the finish rate, defined as the proportion of missing pieces successfully placed. The sampling method involves comparing pairs of target locations and iteratively selecting the better option until a single target location remains. We guarantee that the correct answer exists within the sampling process. In our method, once a jigsaw piece is moved to the imagined target location, it is considered to be placed. GPT-4o and o1 select the target location by outputting coordinates, while VCoT

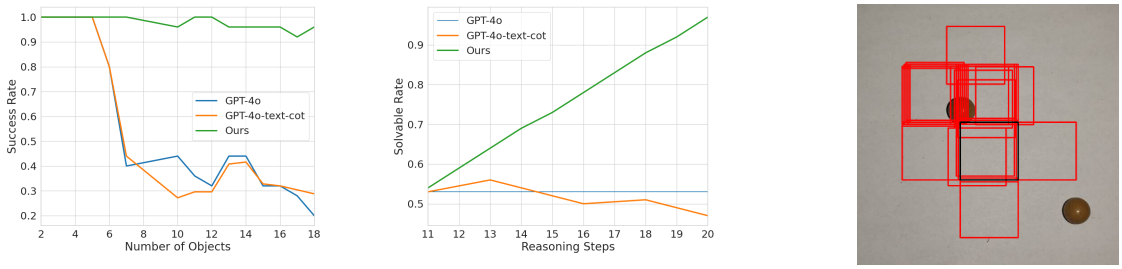

(a) Success Rate vs. Number of Objects (b) Solvable Rate vs. Reasoning Steps (c) Counting by drawing bounding boxes only

Figure 4: (a)(b) show that as counting task difficulty increases linearly, scaling inference-time textual reasoning (implemented as GPT-4o-text-cot, See Sec. 4.3) fails—and even performs worse than vanilla GPT-4o—as complexity exceeds perception limits. In contrast, our methods remain unaffected by these limits, achieving correct counting even as difficulty rises. Additionally, adding visual prompts can introduce noise, causing MLLMs to enter hallucination loops; for instance, in (c), the model incorrectly concluded there were 196 balls when only two were present. The qualitative results of counting are provided in the appendix.

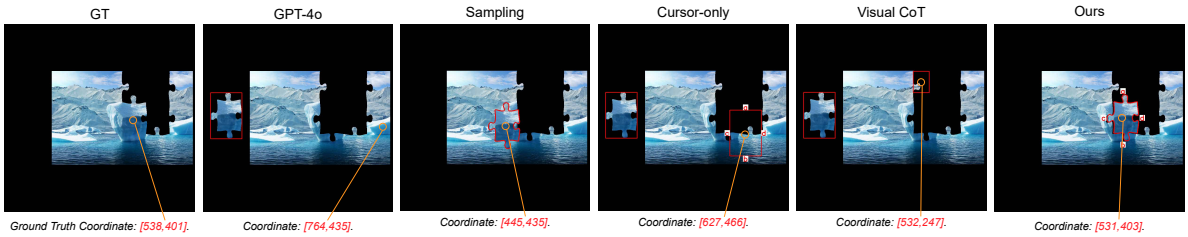

Figure 5: Qualitative comparison on simple jigsaw puzzle solving, we use a black background to make jigsaw pieces more visible to MLLMs. We illustrate the final visual state achieved by different methods after completing their reasoning processes and producing a solution. For clarity, the actual location of each coordinate in the image is highlighted with an orange line and circle.

and Molmo determine the target location by drawing a block or marker, leveraging their specialized training for such tasks.

As shown in Tab. 1 and Fig. 5, our method consistently outperforms all baselines. It achieves a higher locating accuracy, which contributes to a higher success rate with the same number of attempts. Since this visual reasoning task requires the model to choose the correct target location rather than simply locating visible elements, VCoT is ineffective at reasoning. The sampling method performs reasonably well in this task, since we set a large sampling budget to ensure the correct answers can be sampled as the candidate answers. However, despite its extensive reasoning budget, it still does not match the performance of our method. This highlights the effectiveness and robustness of establishing an autonomous perception-control loop. We also demonstrate that the cursor-only baseline performs similarly to primitive GPT-4o in the four-piece missing scenario. However, it performs significantly better under the more challenging six-piece missing scenario, further confirming the effectiveness of our closed-loop control approach.

4.5 Object Placement

Similar to the approach used in solving simple jigsaw puzzles, the methods compared include the following: GPT-4o and o1, which output the target location by specifying coordinates; the sampling method, which iteratively compares sampled results until a single option remains; VCoT and Molmo, which determines placement by drawing blocks or markers; and our method, which outputs the final placement after completing a transformation operation. In line with how related work in robotics handles sampling-based methods (Kapelyukh et al., 2024; Ding et al., 2024), the sampling baseline restricts its search to a subregion

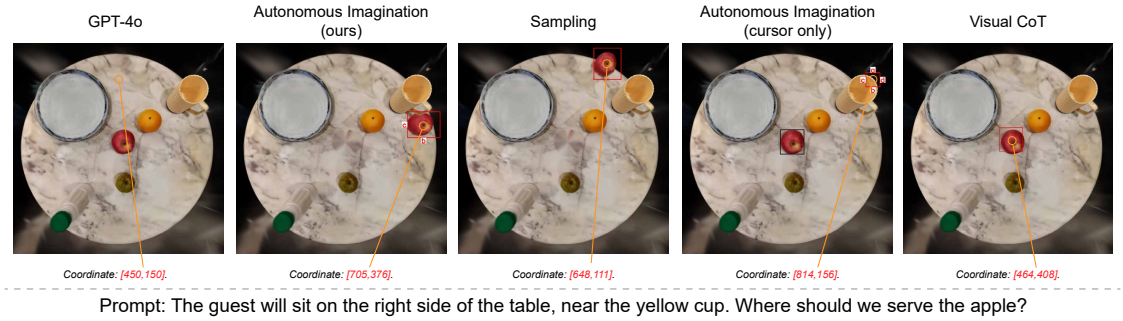

Figure 6: Qualitative comparison of apple placement based on user prompts. Coordinate locations are highlighted on the image with orange lines and circles for improved visualization. Our method aligns more closely with the user's requirements, placing the apple further to the right side of the table.

of the space, filtering out certain incorrect answers. For example, regions occupied by existing objects are excluded from consideration. This principle is also incorporated into the transformation operation in our method. Specifically, a focus operation is first applied to identify the platform on which the target object should reside, creating a region mask. The transformation operation then ensures that no movement is suggested if it would lead the object outside the defined mask. This approach improves efficiency and ensures a fair comparison between the sampling baseline and our method by reducing unnecessary exploration of invalid regions.

As shown in Tab. 1, our method consistently outperforms the baseline methods in both object locating and placement performance. It is important to note that our cursor-only ablation baseline is identical to our full method when locating an object. Therefore, we assign them with the same locating result. Additionally, the sampling method is intractable for locating. Thus, we directly utilize the locating results of our method for placement. Methods lacking advanced visual reasoning capabilities perform poorly on the placement task, as successful placement requires inferencing about the correct spatial position for that element beyond visual recognition. The cursor-only baseline, which moves the visual marker instead of the scene modification, does not perform as effectively as our complete method. This difference underscores the necessity for substantial modification in visual task decomposition. Although the sampling baseline receives substantial visual information, it still underperforms relative to our method and even falls short of the cursor-only baseline. In contrast, in simple jigsaw puzzle solving, the sampling method achieves a relatively high success rate compared to the cursor-only baseline. This contrast highlights the importance of a structured reasoning pathway, particularly in complex, open-world scenarios where the abundant visual information could overwhelm the MLLM, preventing it from identifying the correct answer despite its presence in the sample. By following the closed-loop control reasoning process, MLLMs can progressively approach the correct answer without requiring an exhaustive number of samples, resulting in greater efficiency and improved accuracy.

4.6 Multi-Object Hallucination Benchmark

We evaluated our method using the recently proposed ROPE benchmark for Multi-Object Hallucination (Chen et al., 2024), focusing on the most challenging subset where GPT-4o exhibits the poorest performance, which is answering about a single object given multi-object image, heterogeneous object types, on unseen data split. Our method uses GPT-4o as the base model that equips the imagination space. Please refer to the original paper for more details. Given that this benchmark emphasizes the identification of abstract objects that are not suitable for segmentation, we turn the focus operation into drawing a large rectangular region by MLLMs natively, through selecting top-left and bottom-right corners. The benchmark indicates that MLLMs are prone to hallucinations when confronted with multiple objects that introduce additional visual distractions. We demonstrate that using our method, MLLMs can autonomously focus on the important region despite these distractions, leading to more accurate responses due to the elimination of irrelevant visual information.

Table 2: Results under multi-object hallucination benchmark. Except for o1, Molmo, and our method, the results of other baselines are cited from the official leaderboard in `https://multi-object-hallucination.github.io/`. For each base model family, we take the one with the highest performance. Mechanistically grounded MLLMs (marked with *) take visual prompts by dedicated pointer tokens. Please refer to the original paper for more details.

Models	Acc.	Models	Acc.	Models	Acc.	Models	Acc.
LLaVA-34B	30.81%	CogVLM-C	13.50%	Qwen VL-C	15.37%	Molmo	28.90%
IDEFICS	6.50%	GLaMM*	52.28%	MiniCPM-V	14.39%	o1	60.20%
Yi-VL-34B	0.41%	GroundHOG*	38.13%	GPT-4o	53.74%	GPT-4o+Ours	**65.00%**

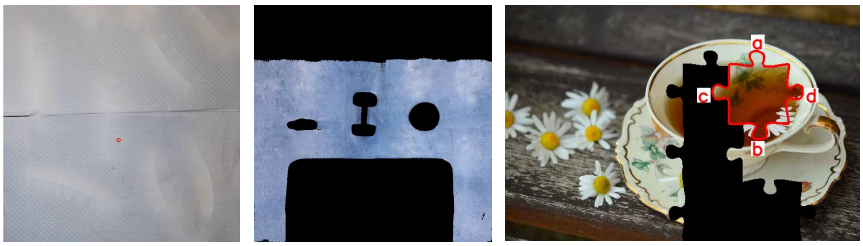

"There is a french fry in the image." "This is the dumbbell." "I should place this piece at this spot."

Figure 7: Failure cases in our method caused by hallucination, including instances where MLLMs mistakenly perceive a fry that does not exist, misinterpret the wrongly focused floor as a dumbbell, and incorrectly believe that a puzzle piece has been placed in the correct spot.

4.7 Discussions

Failure cases. In Fig. 7, we illustrate failure cases of our approach, which are majorly resulted from the hallucination of MLLMs.

Time cost. The time cost of our approach depends mainly on three factors: the running time of a single call of imagination operators, a single call of MLLM reasoning, and the number of MLLM calls. The calls of imagination operators are quite efficient. For example, each call of the SAM model takes 220ms on NVIDIA RTX 4090 on average, which is very efficient compared with MLLM reasoning. Considering the number of calls for MLLM reasoning, the average numbers of MLLM API call for our approach are: counting=117 (for all objects), jigsaw puzzle=20 (for one piece), object placement=15 (for one object), multi-object hallucination=26 (for one object). As shown by the comparisons on GPT-4o Sampling baseline in Tab. 1, our approach is more efficient than previous sampling-based imagination strategies (Kapelyukh et al., 2024; Ding et al., 2024), the closest previous studies to ours, by enabling to solve broader tasks with vast solution spaces.

5 Conclusion

In this work, we target at tackling visual reasoning problems using MLLMs where textual-to-visual conversion is the major bottleneck. We propose the autonomous imagination approach, which employs plug-and-play imagination space and operator design, enabling MLLMs to modify visual content autonomously, leading to closed-loop decomposition of this conversion process. We conduct experiments under visual reasoning tasks that are beyond the perceptual capabilities of MLLMs, while remained straightforward to humans. The results show that these tasks can be effectively tackled natively by MLLMs equipped with our approach.

Limitations and future work. Our work is a proof of concept: while closed-loop task decomposition overcomes the visual-to-textual conversion bottleneck in our demonstrated tasks, resource constraints prevented us from training a model with native closed-loop reasoning and visual modification capabilities. This also prevents us from validating our approach under large, general-purpose visual benchmarks. We hope that our work inspires future efforts to close this critical gap.

References

Anurag Ajay, Seungwook Han, Yilun Du, Shaung Li, Abhi Gupta, Tommi Jaakkola, Josh Tenenbaum, Leslie Kaelbling, Akash Srivastava, and Pulkit Agrawal. Compositional foundation models for hierarchical planning. *arXiv preprint arXiv:2309.08587*, 2023.

Jean-Baptiste Alayrac, Jeff Donahue, Pauline Luc, Antoine Miech, Iain Barr, Yana Hasson, Karel Lenc, Arthur Mensch, Katherine Millican, Malcolm Reynolds, et al. Flamingo: a visual language model for few-shot learning. *Advances in Neural Information Processing Systems*, 35:23716–23736, 2022.

Jinze Bai, Shuai Bai, Shusheng Yang, Shijie Wang, Sinan Tan, Peng Wang, Junyang Lin, Chang Zhou, and Jingren Zhou. Qwen-vl: A versatile vision-language model for understanding, localization, text reading, and beyond. 2023.

Tom Brown, Benjamin Mann, Nick Ryder, Melanie Subbiah, Jared D Kaplan, Prafulla Dhariwal, Arvind Neelakantan, Pranav Shyam, Girish Sastry, Amanda Askell, et al. Language models are few-shot learners. *Advances in neural information processing systems*, 33:1877–1901, 2020.

Keqin Chen, Zhao Zhang, Weili Zeng, Richong Zhang, Feng Zhu, and Rui Zhao. Shikra: Unleashing multimodal llm's referential dialogue magic. *arXiv preprint arXiv:2306.15195*, 2023.

Xi Chen, Xiao Wang, Soravit Changpinyo, AJ Piergiovanni, Piotr Padlewski, Daniel Salz, Sebastian Goodman, Adam Grycner, Basil Mustafa, Lucas Beyer, et al. Pali: A jointly-scaled multilingual language-image model. *arXiv preprint arXiv:2209.06794*, 2022.

Xuweiyi Chen, Ziqiao Ma, Xuejun Zhang, Sihan Xu, Shengyi Qian, Jianing Yang, David Fouhey, and Joyce Chai. Multi-object hallucination in vision language models. In *Advances in Neural Information Processing Systems 37*, 2024.

Matt Deitke, Christopher Clark, Sangho Lee, Rohun Tripathi, Yue Yang, Jae Sung Park, Mohammadreza Salehi, Niklas Muennighoff, Kyle Lo, Luca Soldaini, et al. Molmo and pixmo: Open weights and open data for state-of-the-art multimodal models. *arXiv preprint arXiv:2409.17146*, 2024.

Yufei Ding, Haoran Geng, Chaoyi Xu, Xiaomeng Fang, Jiazhao Zhang, Qiyu Dai, Songlin Wei, Zhizheng Zhang, and He Wang. Open6DOR: Benchmarking open-instruction 6-dof object rearrangement and a VLM-based approach. In *ICRA 2024 Workshop on 3D Visual Representations for Robot Manipulation*, 2024. URL `https://openreview.net/forum?id=axAmAy3Ghl`.

Yilun Du, Mengjiao Yang, Bo Dai, Hanjun Dai, Ofir Nachum, Joshua B Tenenbaum, Dale Schuurmans, and Pieter Abbeel. Learning universal policies via text-guided video generation. *arXiv e-prints*, pp. arXiv–2302, 2023.

Yao Fu, Hao Peng, Ashish Sabharwal, Peter Clark, and Tushar Khot. Complexity-based prompting for multi-step reasoning. In *The Eleventh International Conference on Learning Representations*, 2022.

Wenyi Hong, Weihan Wang, Qingsong Lv, Jiazheng Xu, Wenmeng Yu, Junhui Ji, Yan Wang, Zihan Wang, Yuxiao Dong, Ming Ding, et al. Cogagent: A visual language model for gui agents. *arXiv preprint arXiv:2312.08914*, 2023.

Jie Huang and Kevin Chen-Chuan Chang. Towards reasoning in large language models: A survey, 2023. URL `https://arxiv.org/abs/2212.10403`.

Yuzhou Huang, Liangbin Xie, Xintao Wang, Ziyang Yuan, Xiaodong Cun, Yixiao Ge, Jiantao Zhou, Chao Dong, Rui Huang, Ruimao Zhang, et al. Smartedit: Exploring complex instruction-based image editing with multimodal large language models. In *Proceedings of the IEEE/CVF Conference on Computer Vision and Pattern Recognition*, pp. 8362–8371, 2024.

Itseez. Open source computer vision library. `https://github.com/itseez/opencv`, 2015.

Songtao Jiang, Yan Zhang, Chenyi Zhou, Yeying Jin, Yang Feng, Jian Wu, and Zuozhu Liu. Joint visual and text prompting for improved object-centric perception with multimodal large language models. *arXiv preprint arXiv:2404.04514*, 2024.

Ivan Kapelyukh, Yifei Ren, Ignacio Alzugaray, and Edward Johns. Dream2Real: Zero-shot 3D object rearrangement with vision-language models. In *IEEE International Conference on Robotics and Automation (ICRA)*, 2024.

Bernhard Kerbl, Georgios Kopanas, Thomas Leimkühler, and George Drettakis. 3d gaussian splatting for real-time radiance field rendering. *ACM Transactions on Graphics*, 42(4), July 2023. URL https://repo-sam.inria.fr/fungraph/3d-gaussian-splatting/.

Alexander Kirillov, Eric Mintun, Nikhila Ravi, Hanzi Mao, Chloe Rolland, Laura Gustafson, Tete Xiao, Spencer Whitehead, Alexander C Berg, Wan-Yen Lo, et al. Segment anything. In *Proceedings of the IEEE/CVF International Conference on Computer Vision*, pp. 4015–4026, 2023.

Takeshi Kojima, Shixiang Shane Gu, Machel Reid, Yutaka Matsuo, and Yusuke Iwasawa. Large language models are zero-shot reasoners. *Advances in neural information processing systems*, 35:22199–22213, 2022.

Xin Lai, Zhuotao Tian, Yukang Chen, Yanwei Li, Yuhui Yuan, Shu Liu, and Jiaya Jia. Lisa: Reasoning segmentation via large language model. *arXiv preprint arXiv:2308.00692*, 2023.

Junnan Li, Dongxu Li, Caiming Xiong, and Steven Hoi. Blip: Bootstrapping language-image pre-training for unified vision-language understanding and generation. In *International Conference on Machine Learning*, pp. 12888–12900. PMLR, 2022a.

Junnan Li, Dongxu Li, Silvio Savarese, and Steven Hoi. Blip-2: Bootstrapping language-image pre-training with frozen image encoders and large language models. *arXiv preprint arXiv:2301.12597*, 2023.

Yifei Li, Zeqi Lin, Shizhuo Zhang, Qiang Fu, Bei Chen, Jian-Guang Lou, and Weizhu Chen. On the advance of making language models better reasoners. *arXiv preprint arXiv:2206.02336*, 2022b.

Weifeng Lin, Xinyu Wei, Ruichuan An, Peng Gao, Bocheng Zou, Yulin Luo, Siyuan Huang, Shanghang Zhang, and Hongsheng Li. Draw-and-understand: Leveraging visual prompts to enable mllms to comprehend what you want. *arXiv preprint arXiv:2403.20271*, 2024.

Ziyi Lin, Chris Liu, Renrui Zhang, Peng Gao, Longtian Qiu, Han Xiao, Han Qiu, Chen Lin, Wenqi Shao, Keqin Chen, et al. Sphinx: The joint mixing of weights, tasks, and visual embeddings for multi-modal large language models. *arXiv preprint arXiv:2311.07575*, 2023.

Haotian Liu, Chunyuan Li, Qingyang Wu, and Yong Jae Lee. Visual instruction tuning. In *NeurIPS*, 2023.

Ruibo Liu, Jason Wei, Shixiang Shane Gu, Te-Yen Wu, Soroush Vosoughi, Claire Cui, Denny Zhou, and Andrew M. Dai. Mind's eye: Grounded language model reasoning through simulation, 2022. URL https://arxiv.org/abs/2210.05359.

Pan Lu, Liang Qiu, Kai-Wei Chang, Ying Nian Wu, Song-Chun Zhu, Tanmay Rajpurohit, Peter Clark, and Ashwin Kalyan. Dynamic prompt learning via policy gradient for semi-structured mathematical reasoning. *arXiv preprint arXiv:2209.14610*, 2022.

Gen Luo, Yiyi Zhou, Tianhe Ren, Shengxin Chen, Xiaoshuai Sun, and Rongrong Ji. Cheap and quick: Efficient vision-language instruction tuning for large language models. *Advances in Neural Information Processing Systems*, 36, 2023.

Chancharik Mitra, Brandon Huang, Trevor Darrell, and Roei Herzig. Compositional chain-of-thought prompting for large multimodal models. *arXiv preprint arXiv:2311.17076*, 2023.

OpenAI. Hello GPT-4o, 2024a. URL https://openai.com/index/hello-gpt-4o/.

OpenAI. Learning to reason with llms, 2024b. URL https://openai.com/index/learning-to-reason-with-llms/.

Zhiliang Peng, Wenhui Wang, Li Dong, Yaru Hao, Shaohan Huang, Shuming Ma, and Furu Wei. Kosmos-2: Grounding multimodal large language models to the world. *arXiv preprint arXiv:2306.14824*, 2023.

Ji Qi, Ming Ding, Weihan Wang, Yushi Bai, Qingsong Lv, Wenyi Hong, Bin Xu, Lei Hou, Juanzi Li, Yuxiao Dong, et al. Cogcom: Train large vision-language models diving into details through chain of manipulations. *arXiv preprint arXiv:2402.04236*, 2024.

Nikhila Ravi, Valentin Gabeur, Yuan-Ting Hu, Ronghang Hu, Chaitanya Ryali, Tengyu Ma, Haitham Khedr, Roman Rädle, Chloe Rolland, Laura Gustafson, et al. Sam 2: Segment anything in images and videos. *arXiv preprint arXiv:2408.00714*, 2024.

Ohad Rubin, Jonathan Herzig, and Jonathan Berant. Learning to retrieve prompts for in-context learning. *arXiv preprint arXiv:2112.08633*, 2021.

Hao Shao, Shengju Qian, Han Xiao, Guanglu Song, Zhuofan Zong, Letian Wang, Yu Liu, and Hongsheng Li. Visual cot: Unleashing chain-of-thought reasoning in multi-modal language models. *Advances in Neural Information Processing Systems*, 37, 2024.

Qiuhong Shen, Xingyi Yang, and Xinchao Wang. Flashsplat: 2d to 3d gaussian splatting segmentation solved optimally. In *European Conference on Computer Vision*, pp. 456–472. Springer, 2024.

Yongliang Shen, Kaitao Song, Xu Tan, Dongsheng Li, Weiming Lu, and Yueting Zhuang. Hugginggpt: Solving ai tasks with chatgpt and its friends in hugging face. *Advances in Neural Information Processing Systems*, 36, 2023.

Weihan Wang, Qingsong Lv, Wenmeng Yu, Wenyi Hong, Ji Qi, Yan Wang, Junhui Ji, Zhuoyi Yang, Lei Zhao, Xixuan Song, et al. Cogvlm: Visual expert for pretrained language models. *arXiv preprint arXiv:2311.03079*, 2023a.

Wenhai Wang, Zhe Chen, Xiaokang Chen, Jiannan Wu, Xizhou Zhu, Gang Zeng, Ping Luo, Tong Lu, Jie Zhou, Yu Qiao, et al. Visionllm: Large language model is also an open-ended decoder for vision-centric tasks. *Advances in Neural Information Processing Systems*, 36, 2023b.

Xuezhi Wang, Jason Wei, Dale Schuurmans, Quoc Le, Ed Chi, Sharan Narang, Aakanksha Chowdhery, and Denny Zhou. Self-consistency improves chain of thought reasoning in language models. *arXiv preprint arXiv:2203.11171*, 2022.

Jason Wei, Xuezhi Wang, Dale Schuurmans, Maarten Bosma, Fei Xia, Ed Chi, Quoc V Le, Denny Zhou, et al. Chain-of-thought prompting elicits reasoning in large language models. *Advances in neural information processing systems*, 35:24824–24837, 2022.

Chenfei Wu, Shengming Yin, Weizhen Qi, Xiaodong Wang, Zecheng Tang, and Nan Duan. Visual chatgpt: Talking, drawing and editing with visual foundation models. *arXiv preprint arXiv:2303.04671*, 2023.

Junda Wu, Zhehao Zhang, Yu Xia, Xintong Li, Zhaoyang Xia, Aaron Chang, Tong Yu, Sungchul Kim, Ryan A Rossi, Ruiyi Zhang, et al. Visual prompting in multimodal large language models: A survey. *arXiv preprint arXiv:2409.15310*, 2024a.

Penghao Wu and Saining Xie. V*: Guided visual search as a core mechanism in multimodal llms. *arXiv preprint arXiv:2312.14135*, 17, 2023.

Wenshan Wu, Shaoguang Mao, Yadong Zhang, Yan Xia, Li Dong, Lei Cui, and Furu Wei. Visualization-of-thought elicits spatial reasoning in large language models. *arXiv preprint arXiv:2404.03622*, 2024b.

Zhengyuan Yang, Linjie Li, Jianfeng Wang, Kevin Lin, Ehsan Azarnasab, Faisal Ahmed, Zicheng Liu, Ce Liu, Michael Zeng, and Lijuan Wang. Mm-react: Prompting chatgpt for multimodal reasoning and action. *arXiv preprint arXiv:2303.11381*, 2023.

Shunyu Yao, Dian Yu, Jeffrey Zhao, Izhak Shafran, Thomas L. Griffiths, Yuan Cao, and Karthik Narasimhan. Tree of thoughts: Deliberate problem solving with large language models, 2023. URL https://arxiv.org/abs/2305.10601.

Mingqiao Ye, Martin Danelljan, Fisher Yu, and Lei Ke. Gaussian grouping: Segment and edit anything in 3d scenes. In *European Conference on Computer Vision*, pp. 162–179. Springer, 2024.

Runpeng Yu, Weihao Yu, and Xinchao Wang. Api: Attention prompting on image for large vision-language models, 2024.

Daoan Zhang, Junming Yang, Hanjia Lyu, Zijian Jin, Yuan Yao, Mingkai Chen, and Jiebo Luo. Cocot: Contrastive chain-of-thought prompting for large multimodal models with multiple image inputs. *arXiv preprint arXiv:2401.02582*, 2024.

Shilong Zhang, Peize Sun, Shoufa Chen, Min Xiao, Wenqi Shao, Wenwei Zhang, Kai Chen, and Ping Luo. Gpt4roi: Instruction tuning large language model on region-of-interest. *arXiv preprint arXiv:2307.03601*, 2023a.

Yuanhan Zhang, Kaiyang Zhou, and Ziwei Liu. What makes good examples for visual in-context learning? *Advances in Neural Information Processing Systems*, 2023b.

Yuechen Zhang, Shengju Qian, Bohao Peng, Shu Liu, and Jiaya Jia. Prompt highlighter: Interactive control for multi-modal llms. *arXiv preprint arXiv:2312.04302*, 2023c.

Zhuosheng Zhang, Aston Zhang, Mu Li, and Alex Smola. Automatic chain of thought prompting in large language models. *arXiv preprint arXiv:2210.03493*, 2022.

Zhuosheng Zhang, Aston Zhang, Mu Li, Hai Zhao, George Karypis, and Alex Smola. Multimodal chain-of-thought reasoning in language models. *arXiv preprint arXiv:2302.00923*, 2023d.

Ge Zheng, Bin Yang, Jiajin Tang, Hong-Yu Zhou, and Sibei Yang. Ddcot: Duty-distinct chain-of-thought prompting for multimodal reasoning in language models. *Advances in Neural Information Processing Systems*, 36:5168–5191, 2023.

Enshen Zhou, Yiran Qin, Zhenfei Yin, Yuzhou Huang, Ruimao Zhang, Lu Sheng, Yu Qiao, and Jing Shao. Minedreamer: Learning to follow instructions via chain-of-imagination for simulated-world control. *arXiv preprint arXiv:2403.12037*, 2024a.

Qiji Zhou, Ruochen Zhou, Zike Hu, Panzhong Lu, Siyang Gao, and Yue Zhang. Image-of-thought prompting for visual reasoning refinement in multimodal large language models, 2024b. URL https://arxiv.org/abs/2405.13872.

Yiyi Zhou, Tianhe Ren, Chaoyang Zhu, Xiaoshuai Sun, Jianzhuang Liu, Xinghao Ding, Mingliang Xu, and Rongrong Ji. Trar: Routing the attention spans in transformer for visual question answering. In *Proceedings of the IEEE/CVF international conference on computer vision*, pp. 2074–2084, 2021.

Deyao Zhu, Jun Chen, Xiaoqian Shen, Xiang Li, and Mohamed Elhoseiny. Minigpt-4: Enhancing vision-language understanding with advanced large language models. *arXiv preprint arXiv:2304.10592*, 2023.

Zhuofan Zong, Bingqi Ma, Dazhong Shen, Guanglu Song, Hao Shao, Dongzhi Jiang, Hongsheng Li, and Yu Liu. Mova: Adapting mixture of vision experts to multimodal context. *arXiv preprint arXiv:2404.13046*, 2024.

Table 3: Quantitative results on counting using CogCoM (Qi et al., 2024), by directly asking it to output the number of objects, and by prompting it to use the trained GROUNDING ability, which counts for the object. We find that though explicitly trained to perform GROUNDING which counts the specific object, it somehow performs worse in our evaluation.

Settings		CogCoM	CogCoM-GROUNDING
Counting	Success Rate	30.3%	14.8%
	Mean Error	1.26	3.77
	Variance	1.39	15.47

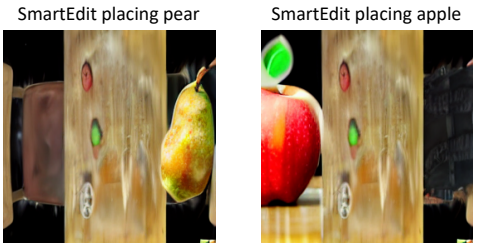

Figure 8: We show that existing image editing models lack the capability to effectively comprehend and execute complex commands, such as placing the apple/pear at the left/right side on the table.

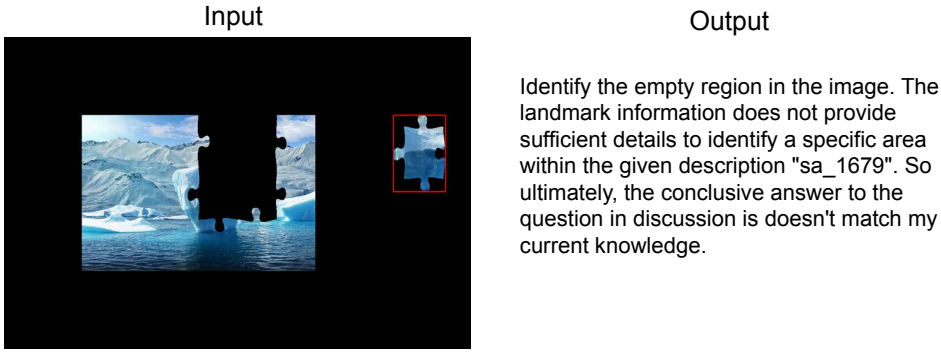

Figure 9: Qualitative results on using CogCoM (Qi et al., 2024) for jigsaw puzzle solving show that it generates unrelated text when asked where the highlighted puzzle piece should be placed.

A More Experiments

Imagine with Image Editing Models. We experimented with utilizing image editing models that accept input of natural languages, such as the state-of-the-art model SmartEdit (Huang et al., 2024). Ideally, such models would provide effective guidance by generating the target goal based on descriptions in natural language. However, as shown in Fig. 8, we find that the image editing model is not ideal when it comes to following complex instructions. This underscores the significant challenge of "imagining" the target state in open-world problems, suggesting that a world model capable of accurately providing such visual guidance requires further development.

CogCoM. We have also experimented with a potentially feasible baseline CogCoM (Qi et al., 2024). However, we find that it does not function well when tackling our challenges. Despite explicitly trained with a GROUNDING ability for counting objects, as shown in Tab. 3, directly prompting the model to output the counting result is more accurate than performing GROUNDING. When asked to complete the jigsaw puzzle by finding target location, it starts hallucinating by outputing unrelated text, as shown in Fig. 9. This is potentially due to the model trained on different tasks and not generalizing to our challenged tasks. We decided to present the result in the appendix instead.

B Additional Qualitative Results

We present qualitative results on tasks that include counting, solving simple jigsaw puzzles, and placing objects in Fig. 10 - 14. These images more effectively illustrate the detailed visual reasoning processes and the changes within the imagination space. Please also see the supplementary video, which shows the reasoning process of our approach in the jigsaw puzzle solving task.

C System Prompts

We provide system prompts for the reasoning instructions given to the MLLMs in our tasks, as shown in Fig. 15, as well as the prompts used as reminders for autonomous imagination operations, as illustrated in Fig. 16. We will make our code publicly available upon acceptance.

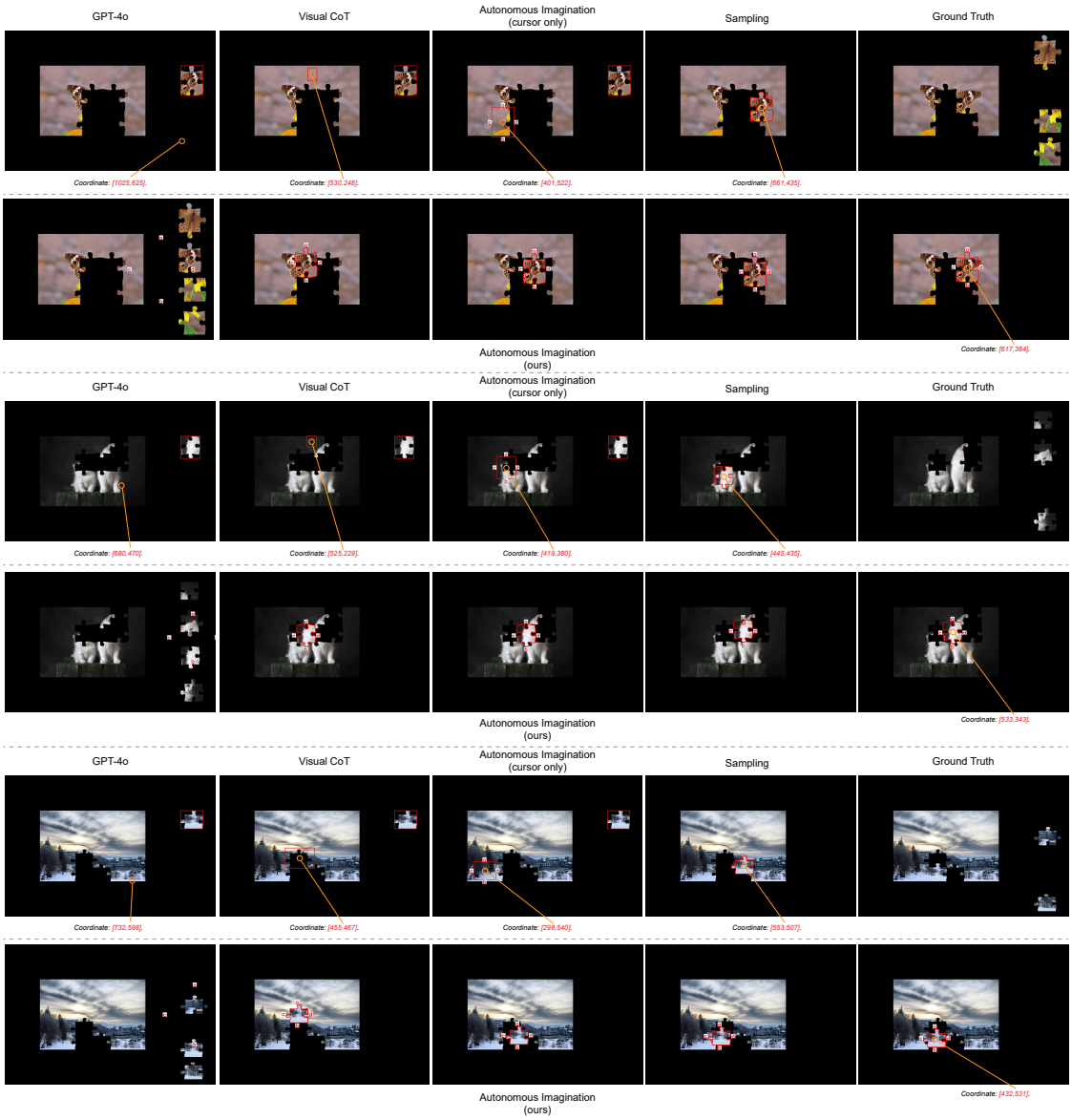

Figure 10: Additional qualitative results of simple puzzle solving. Please zoom in for a clearer view.

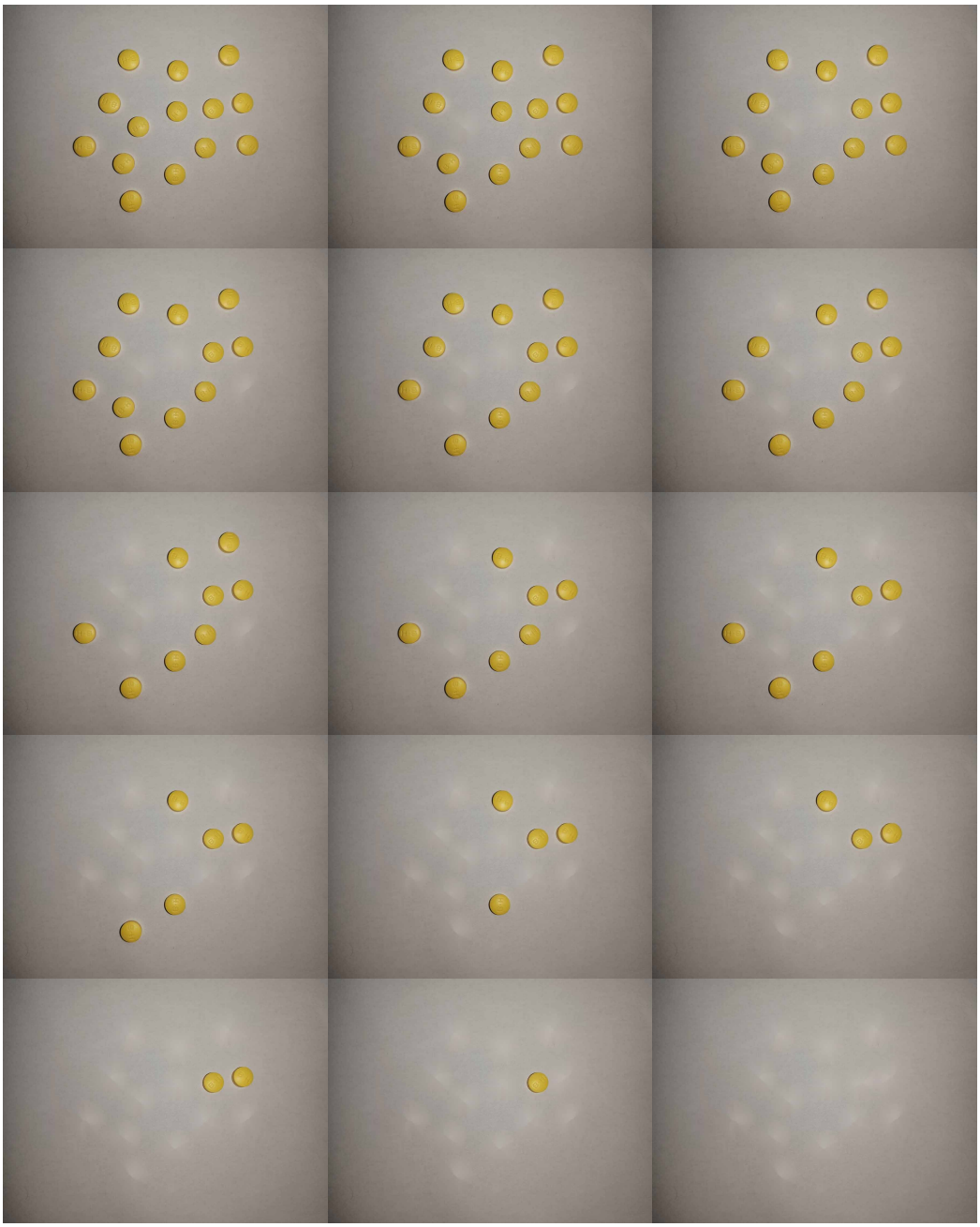

Figure 11: Qualitative demonstration of the counting process autonomously performed by our approach.

Figure 12: Qualitative demonstration of the counting process autonomously performed by our approach.

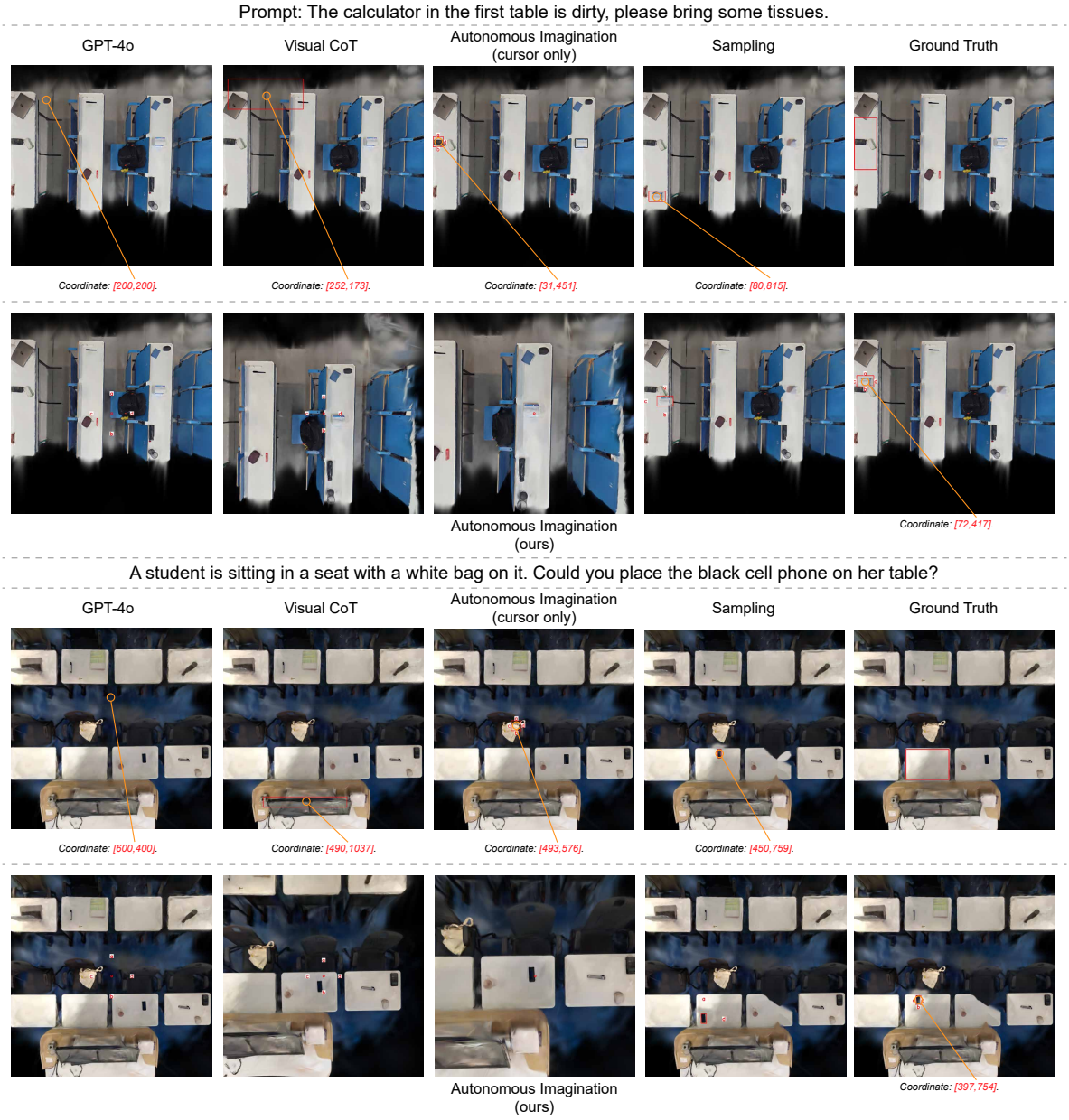

Figure 13: Additional qualitative results of object placement are provided. We also illustrate some steps in our method during the search for the target object and its placement. Please zoom in for a clearer view.

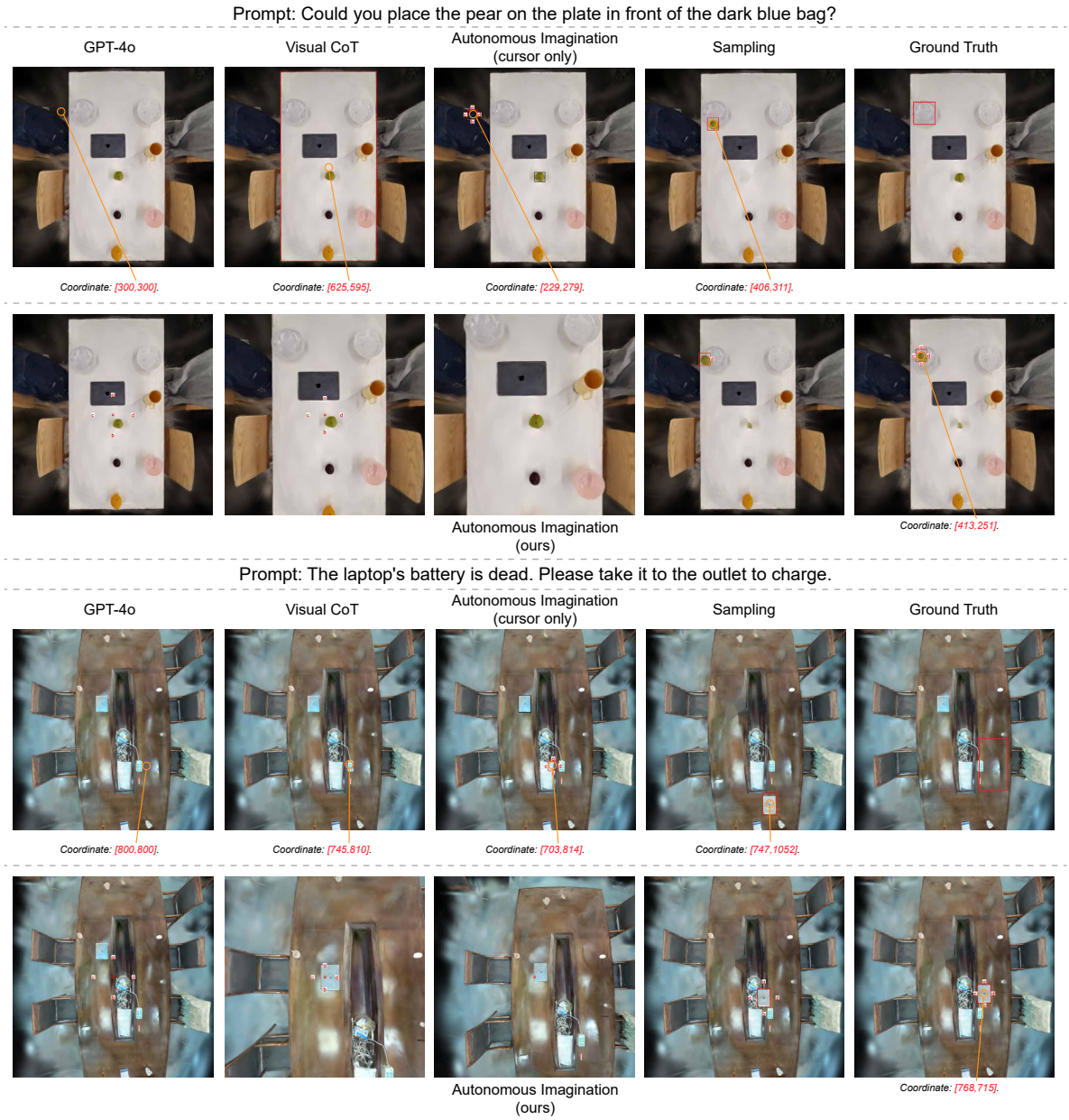

Figure 14: Additional qualitative results of object placement are provided. Please zoom in for a clearer view.

General Reasoning Instructions for Counting
You are an assistant which counts the number of specific objects in the given image and outputs it. Please recognize distinct objects one by one, describe each unique object including its color and location, and count during this process.

General Reasoning Instructions for Jigsaw Puzzle Solving
In this task, you will receive a picture of an unfinished puzzle. The image contains a nearly complete puzzle and several pieces that have not yet been placed into the whole.

You should think step by step as follows:
1. Which of these individual puzzle pieces fits best into the whole? Describe the contents and location of the puzzle piece.
2. Establish a two-dimensional rectangular coordinate system in the image, with the lower left corner as the origin, the right direction as the positive x-axis, and upward as the positive y-axis. The x-axis coordinate range of the image is 0~$IMAGE_WIDTH (pixels), and the y-axis coordinate range is 0~$IMAGE_HEIGHT (pixels).

Please output the coordinates of your selected piece in the image. You should output the answer in the last line in the format ['x_coordinate','y_coordinate'].

General Reasoning Instructions for Object Placement
You are an assistant that decides where to place an object based on user requirements.
First, make a plan by:
1. Listing the objects mentioned in the user requirement
2. Identifying which objects need to be moved or placed
3. Determining a reasonable order to move them

Finally, summarize the objects with numbers that need to be moved in the last line, using lowercase singular form. The output format should be [['Object', Object_number]].

A two-dimensional rectangular coordinate system is established in the image, with the lower left corner as the origin (right = positive x-axis, upward = positive y-axis). The x-axis ranges 0~$IMAGE_WIDTH (pixels), and y-axis ranges 0~$IMAGE_HEIGHT (pixels).

For each object:
1. Locate it by outputting its coordinates
2. Output the target location coordinates

You should format your final answer as ['x_coordinate','y_coordinate'].

Prompts for Autonomous Imagination
You can manipulate the scene using these operations:
1. Control a cursor to focus on objects
2. Transform focused objects or ignore them
3. Return to cursor control after operations

For counting: Ignore irrelevant objects while counting.
For object placement: Move the cursor to focus on the target object, then transform it to the proper location.
For jigsaw puzzles: Focus on the puzzle piece and transform it to its ideal position.

Figure 15: General reasoning instructions provided to models for visual reasoning, as well as the reasoning instruction given to utilize autonomous imagination. It is not difficult for an advanced MLLM to figure out this plan. As we aim to break the visual-to-textual conversion bottleneck, we simplify this by directly given the reasoning plan to the MLLM to avoid occasional failure caused by the MLLM choosing a bad reasoning strategy.

Cursor Control
You are now controlling the cursor. You should find the target object based on the plan you made. You will receive an image and the object to be located. There is a red circle in the image, surrounded by the four letters: 'a', 'b', 'c', and 'd'. You should choose the letter closest to the target object. If there are multiple target objects in the image, you should aim the red circle at the closest one. Ignore artifacts like shadows and floating spots. You should output the quoted letters in the last line, that is: ['a'], ['b'], ['c'], or ['d']. The distance will be reduced in each iteration until convergence, so you only need to choose the direction.

Checking Focus Segmentation
Your task is to check if the object shown in the image is the object you seek. The image should show a single target object against a black background. Areas of the image that do not belong to the object are set to black. If not, you should judge it as ['no'] and end your check. You should imagine what the object would look like from above and compare it to the image.

You should describe the object in the image, then output the check result in the last line in the format: ['yes'] or ['no'].

After Focus
You are now focusing on the object you desire. You can choose to perform a transform operation or ignore the operation based on your own plan. Output ['transform'] or ['ignore'] in the last line to perform the corresponding operation.

Transform Control
You are now moving the object to the destination. The object you are controlling is highlighted and surrounded by at most four letters: 'a', 'b', 'c', and 'd'. Ignore artifacts like shadows and floating spots. Choose the direction leading to the destination. The distance will be reduced in each iteration until convergence, so you only need to choose the direction. You should output the quoted letters in the last line, that is: ['a'], ['b'], ['c'], or ['d'].

Cursor Control (Special Focus for Multi-Object Hallucination)
You are now controlling the cursor. You should focus on the region based on the provided object ID. You should first move the cursor to the top-left corner of the object region. There is a red circle in the image, surrounded by the four letters: 'a', 'b', 'c', and 'd'. You should output the quoted letters in the last line, that is: ['a'], ['b'], ['c'], or ['d']. The distance will be reduced in each iteration until convergence, so you only need to choose the direction.

You have selected the top-left corner of the region. You should focus on the bottom-right corner of the region to be focused on. There is a red circle in the image, surrounded by the four letters: 'a', 'b', 'c', and 'd'. You should output the quoted letters in the last line, that is: ['a'], ['b'], ['c'], or ['d']. The distance will be reduced in each iteration until convergence, so you only need to choose the direction.

Figure 16: Detailed prompts instructing the MLLM about the operations it can utilize. This is given to the MLLM as a reminder when the MLLM enters corresponding state during the reasoning.